# PP/Clay Nanocomposites: Effect of Clay Treatment on Morphology and Dynamic Mechanical Properties

**PRAVIN KODGIRE,*  RAJENDRA KALGAONKAR,  SANGEETA HAMBIR,  NEELIMA BULAKH,  J. P. JOG**

Chemical Engineering Division, National Chemical Laboratory, Pune 411 008, India

**ABSTRACT:** The morphology and properties of polypropylene (PP)/clay nanocomposites are described. The melt intercalation of organophilic clay was carried out with a single-screw extruder. The effects of two kinds of treatments of clay are discussed. Maleic anhydride (MAH)-grafted PP was used as a compatibilizer. The expansion of the intergallery distance of the clay was governed by the interaction between the clay treatment and the compatibilizer. In one case, the composites exhibited significantly reduced intensities of diffraction peaks, suggesting partial exfoliation of the clay layers, whereas for the second clay sample, expansion of the gallery height was noted. The mechanical properties of the PP/clay composites showed significant enhancement in their mechanical and thermal properties. About a 35% increase in the tensile modulus and about a 10% increase in the tensile strength were observed. The thermal degradation temperature increased from 270 to about 400°C as a result of the incorporation of clay, and the extent depended on the dispersion of clay in the composite. The most interesting outcome of this study was the changes in morphology for PP/clay composites, which are reported here for the first time. An optical microscopic study revealed that the PP/clay composites could be crystallized at higher temperatures than pure PP and that the morphology was remarkably altered because of the presence of layers of clay. © 2001 John Wiley & Sons, Inc. J Appl Polym Sci 81: 1786–1792, 2001

**Key words:** PP; clay; nanocomposites; DMA

## INTRODUCTION

Nanocomposites are an emerging area of contemporary research and have received a great deal of attention. Nanocomposites exhibit unexpected hybrid properties. A large number of scientists are looking at various aspects of these composites.

Nanocomposites based on clay are increasingly being developed and studied. The process of creating these nanocomposites involves intercalation of organic compounds into the clay layers, resulting in an expanded and organophilic layered structure. This organophilic clay is then incorporated into the polymer matrix via *in situ* polymerization or melt intercalation. This process provides dispersion of the clay in the polymer matrix and leads to significant improvements in its mechanical properties.[1–6] These new materials can satisfy the ever-demanding requirements of materials for high-technology applications. Nylon-based composites have even been commercialized.

Polypropylene (PP)/clay composites are interesting because of their possible applications in the automobile industry. There have been few articles on PP/clay nanocomposites by a group from Toyota.[7–9] The dispersability and dynamic me-

*Correspondence to:* J. P. Jog (jyoti@che.ncl.res.in).
*\*Present address:* Chemical Engineering Department, Faculty of Technology and Engineering, Maharaja Sayajirao University of Baroda, Vadodara 390001, India.

chanical properties of PP composites with strearyl-amine-treated clay and mica with maleic anhydride (MAH)-grafted PP oligomers as compatibilizers have been discussed.

In this article, we present results on the morphology and properties of PP/clay composites. Two organophilic clays with different cation-exchange capacities (CECs) and treatments were used. The effects of the type of clay on the properties of the PP/clay composites are compared.

## EXPERIMENTAL

### Materials

PP (grade M0030) used for this study was procured from IPCL (Vadodara, India). The MAH-modified PP (grade 3150) was procured from BP Chemicals (Hackettstown, NJ).

Two organically modified montmorillonite clay samples were used in this study, Cloisite (6A), generously donated by Southern Clay Products (Gonzales, TX), and Nanocor (N1) donated by Nanocor Inc. (Arlington Heights, IL). The montmorillonite was organically modified with a tallow compound (for Southern Clay Products clay) and octadecylamine (for nanocor clay). The CEC values for the two clay samples were reported to be 140 and 135 meq/100 g, respectively.

### Preparation of the Composites

The melt compounding of PP/clay composites was carried out with a Brabender (Duisburg, Germany) single-screw extruder. The clay and polymer samples were dried in an air circulatory oven at 65°C for 8 h prior to compounding.

The temperature zones ranged from 160 to 200°C, and the revolutions-per-minute rate was 45. One composition containing polymer (84%), compatibilizer (12%), and clay (4%) was prepared for each clay.

The specimens for mechanical testing were prepared with a Morgan (Long Beach, CA) model G-100T press. The films for X-ray diffraction (XRD) analysis were prepared with a Carver (Menomonee Falls, WI) model F-15181 press.

### XRD

The dispersability of clay in the polymer matrix was evaluated with X-ray diffractometer measurements, which were carried out with a Rigaku (The Woodlands, TX) model Dmax 2500 instrument with Cu K$\alpha$ radiation. The basal spacing of the montmorillonite (MMT) was estimated from the (001) peak in the XRD pattern.

### Thermogravimetric Analysis (TGA)

TGA was done with a Seiko (Torrance, CA) model TG/DTA 32 thermal analysis system. The TGA scans were recorded at 10°C /min under a nitrogen atmosphere from room temperature to 900°C.

### Dynamic Mechanical Analysis (DMA)

Dynamic mechanical properties of the samples were studied on compression-molded films with a Rheometrics (Piscataway, NJ) model IIIE dynamic mechanical analyzer in the tensile mode. The samples were tested from −40 to 140°C and at a frequency of 10 rad/s. The temperature sweep was carried out in the auto-strain mode.

### Mechanical Testing

Tensile testing was carried out at a crosshead speed of 50 mm/min with an Instron (High Wycombe, UK) 4204 Universal Testing Machine equipped with an incremental extensometer. Young's modulus, tensile strength, and percent elongation were determined from the stress–strain curves as per ASTM D638 sample type IV. The flexural strength and modulus were determined at a crosshead speed of 1.3 mm/min as per ASTM D 790, and the strength was determined at a 5-mm displacement.

### Optical Microscopy (OM)

The spherulitic morphology of PP and PP/clay composites was studied with a Leica (Heerbrugg, Switzerland) Laborlux 12 Pol S equipped with an attachment named *microvid*. The samples were prepared by the melt pressing of the PP and PP/clay composites at 200°C between a glass slide and a cover slip; they were kept at this temperature for 1 min to ensure uniform melting. The slides were then transferred to the hot stage and isothermally crystallized at 122 and 142°C. The photomicrographs were taken under cross polarizers with a Leica Wild MPS 52 with an automatic-exposure unit.

## RESULTS AND DISCUSSION

### XRD

Figure 1 shows the XRD patterns for the clay samples used and the PP/clay composites. The
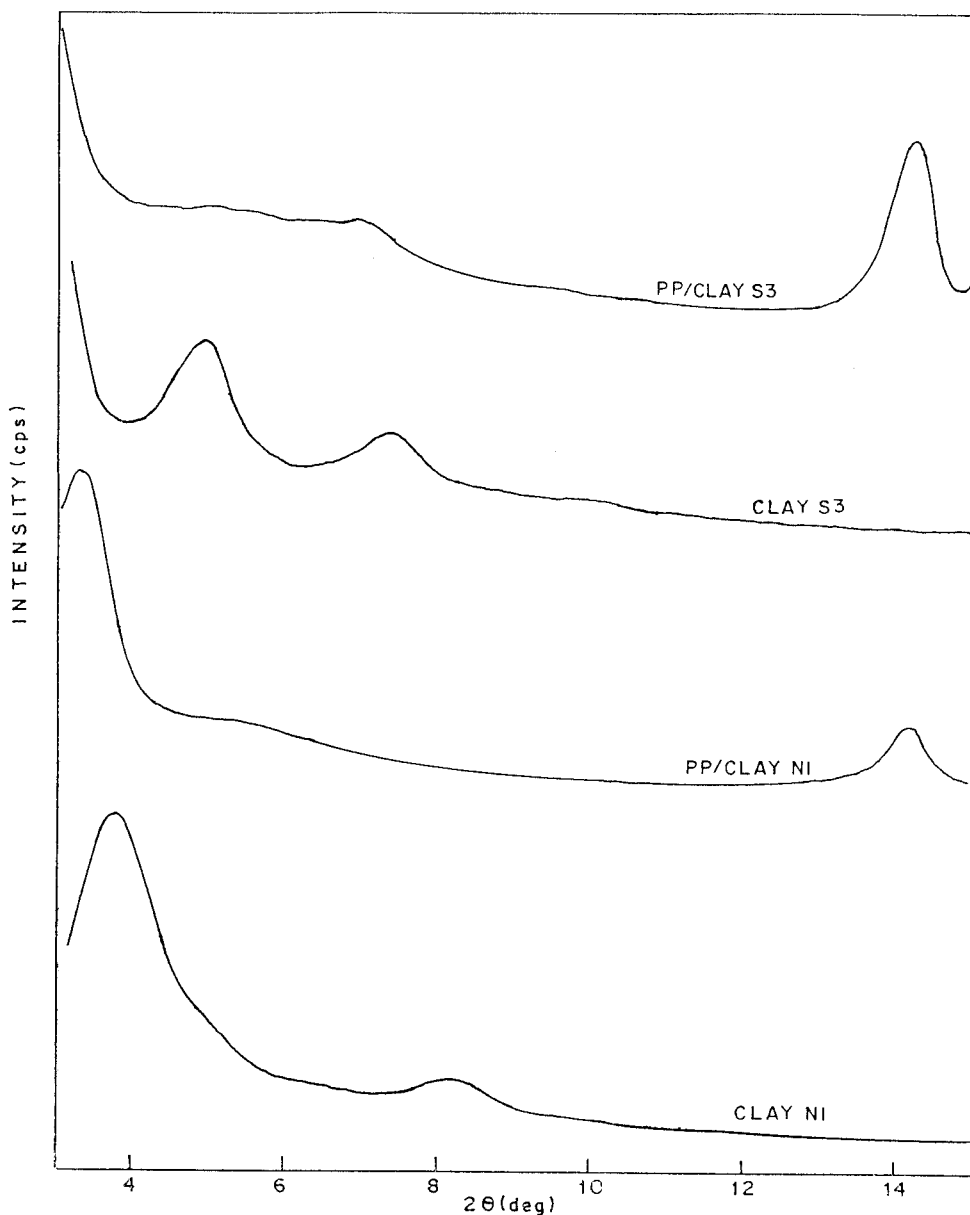
**Figure 1** XRD scans of clay and PP/clay composites.

$Na^+$ MMT exhibits a single peak at about 7.8°, corresponding to basal spacing of 12 Å. As can be seen from Figure 1, the treatment of clay resulted in an intercalation and thus a shift in the peak to lower $2\theta$ values (i.e., larger basal spacing).

The sample clay 6A showed two characteristic peaks at $2\theta$ values of 7 and 4.5°, corresponding to basal spacings of 12 and 18 Å, respectively. The presence of two peaks in sample 6A indicated the presence of heterostructures in the clay caused by organic and inorganic layers. This could occur when the inorganic cations of smectic clays are partially replaced by organic ions. This is possi-

ble, as the CEC of the sample was much higher (140 meq/100 g). The presence of such hetero-structures was reported by Ijdo and Pinnavaia.[6] For the nanocor sample, only one peak at $2\theta$ values of about 4. 0° was observed, corresponding to a basal spacing of 24.5 Å. This finite expansion of the gallery height is associated with the interca-lation of clay.

Figure 2 shows the XRD pattern of the PP/clay composites. As shown in the figure, the PP/clay 6A composite showed remarkable changes in the X-ray patterns. The composites of clay 6 A with PP showed that the intensity of the two peaks

decreased significantly. This indicates a decrease in the degree of coherent layer stacking caused by a more disordered structure.

In the PP/clay nanocor composites, this peak shifted to $2\theta$ values of about 3.0°, corresponding to a basal spacing of 27 Å. The presence of this peak indicates that the clay was not delaminated; instead, the gallery height was increased by about 0.3 nm as a result of PP intercalation. The increased intensity of the diffraction peak suggests coherent stacking of the clay platelets and, thus, the presence of an ordered structure.

The expansion of the intergallery distance of the clay was governed by the interaction between the clay treatment and the compatibilizer. In one case, the composites exhibited the disappearance of the diffraction peaks, confirming the exfoliation of the clay layers, whereas for the second clay sample, a marginal change was observed. This difference in the X-ray patterns of the two composites may have been caused by the difference in the treatments of the clay. As was reported earlier, the dispersability of the clay in the polymer was dependent on the interaction of the treatments used for modifying the clay and the polymer. In this case, sample 6A was treated with a tallow compound, whereas the nanocor sample was treated with octadecylamine. The dispersability of the clay in the composites in the case of tallow treatment showed delamination; on the other hand, marginal expansion of the clay platelets was observed in the case of clay treated with octadecylamine.
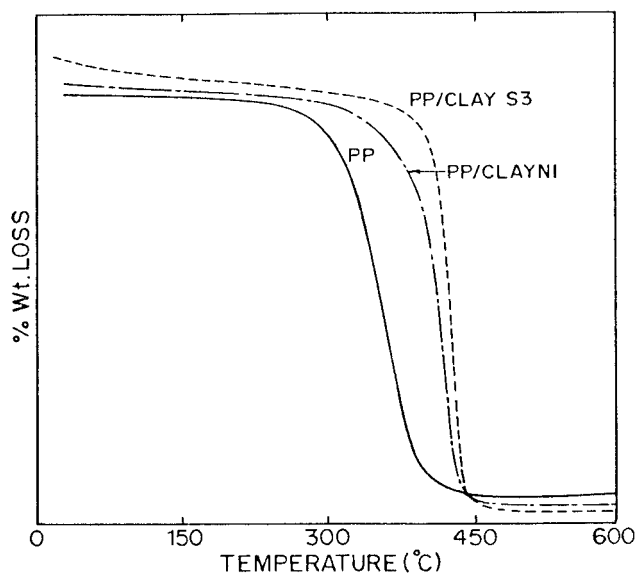
**Table I    Percent Weight Loss of the Two Clay Samples at Various Temperatures**

| Sample | Percent Weight Loss | | |
| --- | --- | --- | --- |
| | 140 (°C) | 614 (°C) | 875 (°C) |
| Cloisite® 6A | 0.72 | 43.4 | 48.2 |
| Nanocor | 0.78 | 32.6 | 36.4 |

## TGA

Table I presents the percent weight loss at three temperatures for the clay samples. The weight loss at 140°C corresponded to the weight loss caused by surface hydration. The two clay samples exhibited different values of percent weight loss at 140°C, which may be attributed to the hydrophilic/hydrophobic nature of the clay, which was determined by the treatment. The percent weight loss at about 600°C showed remarkable differences between the two clays. This weight loss was caused by the degradation of organic onium and, thus, indicated the level of intercalation. Sample 6A contained more organic matter than the nanocor sample.

Figure 2 shows the TGA scans of PP and PP/clay composites. The incorporation of clay in a platelet form resulted in a significant improvement in the thermal stability of PP. The temperature at the onset of degradation increased from about 270 to about 330 and 400°C for clay 6A and nanocor samples, respectively. For the PP/nanocor sample, the enhancement in the thermal stability was about 60°C, whereas for the PP/6A sample, the increase was about 130°C. A similar increase in the thermal stability has already been reported for polystyrere (PS)/clay, poly(dimethyl siloxane) (PDMS)/clay, poly(methyl methacrylate)/clay, poly(ethylene terephthalate) (PET)/clay, and epoxy/magadiite composites.[10–14] The enhancement in the thermal stability of the polymer/clay composites has been attributed to the decreased permeability of oxygen caused by the exfoliated clay in polymer/clay composites.

## OM

PP is known to exhibit a well-defined spherulitic morphology when crystallized from melt. Figures 3(a) and 3(b) show the optical micrographs of the PP sample crystallized at 122°C at the early stage and the final stage of PP crystallization; the micrographs exhibit the well-defined spherulitic
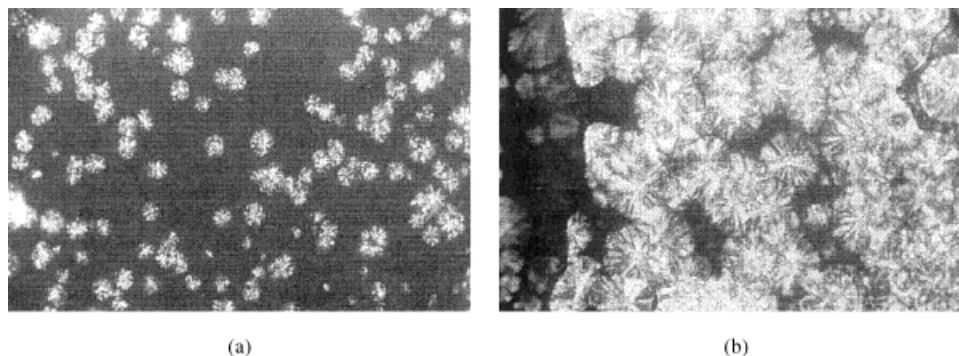


**Figure 2**    TGA scans of clay and PP/clay composites.

**Figure 3** (a) Optical micrographs of PP spherulites crystallized at 122°C for 10 min (10×). (b) Optical micrographs of PP spherulites crystallized at 122°C for 35 min (10×).

morphology of PP. However, when crystallized at temperatures of about 140°C, PP did not crystallize within an experimental time of about 30 min. In composites, the crystallization of PP took place even at temperatures as high as 142°C and did not exhibit a spherulitic morphology.

Figures 4(a) and 4(b) show the optical micrographs for PP/clay composites crystallized for 35 min at 142°C. In the composites, the crystallites grew as fibers that increased in diameter. Even after a prolonged crystallization time, the morphology of PP remained fibrous and did not show the usual spherulitic behavior. PP did not crystallize at this temperature at all, whereas in the presence of clay, it crystallized in a different form. This indicates that the surface of the exfoliated clay layers acted as a nucleating agent, which promoted the crystallization of PP.

### Mechanical Properties of the PP/Clay Composites

The most important property of nanocomposites is the enhancement in mechanical properties even at low percentages of the clay loading. Table II presents the mechanical properties of the PP/clay composites. As shown in the table, the tensile modulus, flexural strength, and flexural modulus increased as a result of clay incorporation. For the PP/clay 6A sample, the increase in tensile modulus was about 35%, whereas the increase in the strength was about 10%. The flexural properties also showed significant enhancement. The flexural modulus increased by about 30%, whereas the flexural strength increased by 25%. In the case of the PP/nanocor sample, a similar increase was also observed in its mechanical properties. This enhancement in the properties at a clay loading of 4% by weight could be attributed to the exfoliation/expansion of clay platelets in the polymer matrix. Both composites exhibited comparable tensile strength and moduli, although the structure of the composites as determined from XRD indicated intercalation and delamination of clay for the nanocor and 6A samples, respectively. At low clay loadings of about 5 wt %, tensile
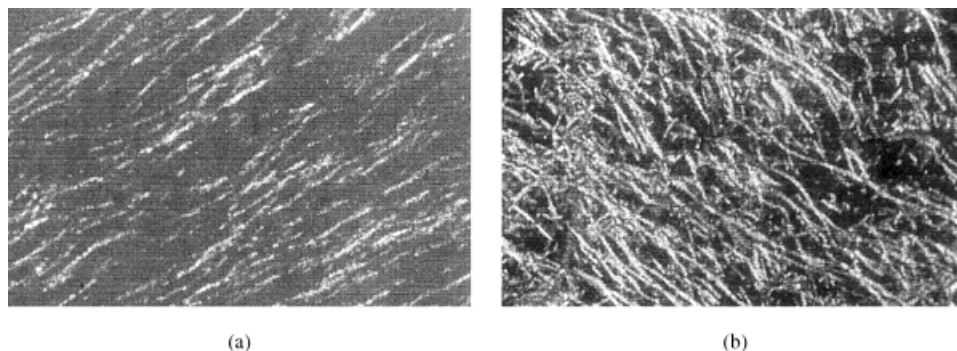


**Figure 4** (a) Optical micrographs of PP/clay 6A composites crystallized at 142°C for 35 min (10×). (b) Optical micrographs of PP/clay nanocor composites crystallized at 142°C for 35 min (10×).

**Table II  Mechanical Properties of the PP/Clay Nanocomposites**

| PP/Clay Composites | Tensile Strength (MPa) | Tensile Modulus (MPa) | Elongation (%) | Flexural Strength (MPa) | Flexural Modulus (MPa) |
|---|---|---|---|---|---|
| PP | 32 | 1450 | 28.2 | 32.3 | 1390 |
| PP/clay 6A | 35.8 | 2028 | 7.7 | 39.9 | 1785 |
| PP/clay N1 | 34.4 | 2067 | 5.4 | 40.9 | 1890 |

properties were comparable, whereas the effect of the delamination of clay platelets was observed at a higher clay loading.[15]

## DMA

DMA is often used to study relaxations in polymers. PP is known to exhibit a glass-transition temperature of about 11°C. An analysis of the storage modulus, loss modulus, and tan δ curves is very useful in ascertaining the performance of samples under stress and temperature. Table III presents the storage modulus for PP and PP/clay composites over a range of temperatures. The PP/clay composite exhibited a higher storage modulus over the entire temperature range of the study (−40 to 120°C). The increase in the storage modulus was about 56%. The loss modulus that corresponded to the dissipation of the energy showed a peak at about 11°C for PP, which corresponds to the glass-transition temperature of PP. For the PP/clay composites, the peak was not well defined as in the case of PP. Also, the loss modulus values were significantly higher than those for PP over the entire temperature range of the study (−40 to 120°C). The two PP/clay composites exhibited a difference in storage moduli. As seen in Table III,

the PP/clay N1 composite exhibited a higher modulus than the PP/clay 6A composite over the entire temperature range. In static mechanical testing, both composites exhibited comparable properties, whereas the dynamic analysis clearly indicates that the intercalated system exhibited a higher storage modulus over the entire range of temperatures studied.

## CONCLUSIONS

The PP/clay nanocomposites exhibited improved mechanical properties at a clay loading of 4% by weight. The tensile modulus increased by about 40%, whereas the tensile strength increased by 10%. The flexural modulus also increased by about 30%, whereas the flexural strength increased by 25%. DMA showed significant improvement in the storage modulus. The extent of the increase was more for PP composites with nanocor clay than for those with 6A clay. The most interesting finding of this study was the dramatic change in morphology observed in the PP/clay composites. The PP/clay composites, when crystallized at a high temperature, exhib-

**Table III  DMA: Storage Modulus of the PP/Clay Composites**

| Temperature (°C) | G′: Storage Modulus (Pa) | | |
|---|---|---|---|
| | PP/Clay 6A | PP/Clay N1 | PP |
| −30 | $2.6728 \times 10^9$ | $3.3123 \times 10^9$ | $2.2695 \times 10^9$ |
| −20 | $2.5736 \times 10^9$ | $3.1342 \times 10^9$ | $2.1976 \times 10^9$ |
| 11 | $1.9567 \times 10^9$ | $2.4281 \times 10^9$ | $1.5489 \times 10^9$ |
| 23 | $1.5621 \times 10^9$ | $2.007 \times 10^9$ | $1.2784 \times 10^9$ |
| 36.6 | $1.3684 \times 10^9$ | $1.803 \times 10^9$ | $1.1133 \times 10^9$ |
| 60.0 | $9.4169 \times 10^8$ | $1.0661 \times 10^9$ | $7.948 \times 10^8$ |
| 80.0 | $6.6880 \times 10^8$ | $7.1859 \times 10^8$ | $5.5013 \times 10^8$ |
| 100.0 | $4.2737 \times 10^8$ | $5.7734 \times 10^8$ | $4.0643 \times 10^8$ |
| 120.0 | $2.6936 \times 10^8$ | $4.2281 \times 10^8$ | $2.8830 \times 10^8$ |

ited peculiar birefringent structures different from the usual spherulites.

## REFERENCES

1. Messersmith, P. B.; Giannelis, E. P. Chem Mater 1994, 6, 1719.
2. Liu, L.; Qi, Z.; Zhu, X. J Appl Polym Sci 1999, 71, 1133.
3. Kojima, Y.; Usuki, A.; Kawasumi, M.; Okada, A.; Fukushima, Y.; Kurauchi, T.; Kamigaito, O. J Mater Res 1993, 8, 1185.
4. Jimenez, G.; Ogata, N.; Kawai, H.; Ogihara, T. J Appl Polym Sci 1997, 64, 2211.
5. Zilg, C.; Mulhaupt, R.; Finter, J. Macromol Chem Phys 1999, 200, 661.
6. Ijdo, W. L.; Pinnavaia, T. J. J Solid State Chem 1998, 139, 281.
7. Kawasumi, M.; Hasegawa, N.; Kato, M.; Usuki, A.; Okada, A. Macromolecules 1997, 30, 6333.
8. Kato, A.; Usuki, A.; Okada, A. J Appl Polym Sci 1997, 66, 1781.
9. Hasegawa, N.; Kawasumi, M.; Kato, M.; Usuki, A.; Okada, A. J Appl Polym Sci 1998, 67, 87.
10. Noh, M. W.; Lee, D. C. Polym Bull 1999, 42, 61.
11. Burnside, S. D.; Giannelis, E. P. Chem Mater 1995, 7, 1597.
12. Lee, D. C.; Jang, L. W. J Appl Polym Sci 1996, 61, 1117.
13. Ke, Y.; Long, C.; Qi, Z. J Appl Polym Sci 1999, 71, 1139.
14. Wang, Z.; Pinnavaia, T. J. Chem Mater 1998, 10, 1820.
15. Pinnavaia, T. J.; Lan, T.; Wang, Z.; Shi, H.; Kaviratna, P. D. ACS Symp Ser 1996, 672, 250.